Proceedings of the
International Conference on Mechanical Engineering 2003
(ICME2003) 26- 28 December 2003, Dhaka, Bangladesh

ICME03-FL-18

A STUDY ON THE PHYSICS OF SUPERSONIC MIXING FIELD WITH INJECTION AT DIFFERENT ANGLES

Mohammad Ali and Shakil Ahmed

Department of Mechanical Engineering
Bangladesh University of Engineering and Technology
Dhaka – 1000, Bangladesh.

ABSTRACT

A numerical study on mixing field of hydrogen and air has been performed by solving two-dimensional full Navier-Stokes equations. An explicit Harten-Yee Non-MUSCL Modified-flux-type TVD scheme has been used to solve the system of equations, and a zero-equation algebraic turbulence model to calculate the eddy viscosity coefficient. The main objective of this study is to study the physics of the flow field and find out the means of increasing the mixing efficiency of a supersonic combustor. The flow field has been studied by varying the hydrogen injection angle made with the direction of air stream. The results show that in upstream of injector the boundary layer is thickened by the backward-facing step and the injection on thick boundary layer enhances mixing. The injection system changes the angles and positions of different shocks in the flow field. Incorporating the various effects, injection with moderate angle shows higher penetration and mixing of hydrogen with air and its large upstream recirculation region has a good flame holding capability.

Keywords: TVD scheme, Backward-facing step, Bow shock, Reattachment shock, Flame holding.

1. INTRODUCTION

The fuel injection scheme in hypersonic vehicles incorporating Scramjet (Supersonic Combustion Ramjet) engines, requires special attention for efficient mixing and stable combustion. Though a considerable number of researches has been carried out on mixing and combustion of fuel with oxidizer in Scramjet program, still it faces many unresolved problems. The main problems that arise in this regard concern mixing of reactants, ignition, flame holding, and completion of combustion. In fact, in supersonic combustion, high penetration and mixing of injectant with main stream is difficult due to their short residence time in combustor as described by Brown et al. [1] and Papamoschou et al. [2]. These investigations showed that good mixing and high penetration of injectant is difficult for the flow of high Mach number. Therefore, it is necessary to investigate the physical mechanisms that affect the mixing and combustion in Scramjet engine.

Several investigations have been performed to analyze the mixing field and increase the mixing efficiency. In these investigations the authors showed a number of parameters that can affect on penetration and mixing. In an experiment, Rogers [3] showed the effect of the ratio between jet dynamic pressure and freestream dynamic pressure on the penetration and mixing of a sonic hydrogen jet injected normal to a Mach 4 airstream. In similar flow arrangements, Kraemer et al. [4] found that the relative change in jet momentum (product of gap width, jet static pressure and injectants specific heat ratio) was directly proportional to the relative size between the flowfield disturbance and the upstream separation distance. The downstream injectant penetration height is directly proportional to the upstream separation distance and thus, the downstream mixing is dependent on the relative change in jet momentum. Similar conclusions were also drawn by Holdeman et al. [5] and Thayer III et al. [6]. Thayer III et al. [6] also found that the injectant concentration of the separated region was high at all conditions investigated. Heister et al. [7] conducted a calculation on the penetration and bow shock shape of a non-reacting liquid jet injected transversely into a supersonic cross flow and obtained a correlation between mass loss, boundary layer thickness, recirculation and related parameters. Ali et al. [8] studied the mixing mechanisms and investigated mixing and combustion characteristics for several flow configurations. On the analysis of mixing the author observed that the backward-facing step in finite flow configuration plays an important role to enhance mixing and penetration in both upstream and downstream of injector. Investigation proved that without diffusion, injectant can spread in the flow field due to species continuity equations, but does not mix with main stream. In another study Ali et al. [9] searched the enhancement of mixing by varying the inlet width of air stream and

found that the flow inlet configuration of a supersonic combustor can play an important role on mixing.

In present investigation, we numerically simulate two-dimensional mixing flow fields for different injecting angles and study the flow field characteristics to search better mixing and good flame holding capability in supersonic combustor. The geometric configuration of the calculation domain and the inlet conditions of main and injecting flows are shown in Fig.1. The left boundary consists of a backward-facing step of height 5 mm, which was found most efficient in mixing by Ali et al. [8]. The injector position from left boundary, backward-facing step height and the inlet width of air stream are kept constant. For this study, the injecting angle 'θ' is varied from 30^0 ~ 150^0 with 30^0 interval in anti-clockwise direction and defined as Case 1, 2, 3, 4 and 5 sequentially. The injector position is fixed at 30 mm from left boundary. The inlet conditions of air are used as Weidner et al. [10] except the Mach number. We choose the Mach number 5.0 for the main flow as the test program has been conducted over the flight Mach number range from 3.0 to 7.0 as described by Rausch et al. [11]. The inlet widths of air and side jet are used as Ali et al. [9]. Throughout the study, the grid system consists of 194 nodes in horizontal direction and 121 in transverse direction.

2. MATHEMATICAL MODELING

The unsteady, two-dimensional full Navier-Stokes and species continuity equations have been solved to analyse the mixing flow field of hydrogen and air. Body forces are neglected. These equations can be expressed by

$$\frac{\partial \mathbf{U}}{\partial t} + \frac{\partial \mathbf{F}}{\partial x} + \frac{\partial \mathbf{G}}{\partial y} = \frac{\partial \mathbf{F_v}}{\partial x} + \frac{\partial \mathbf{G_v}}{\partial y}$$

where, $\mathbf{U} = [\rho,\rho u,\rho v,E,\rho Y_i]^T$,

$\mathbf{F} = [\rho u,\rho u^2+p,\rho uv,(E+p)u,\rho Y_i u]^T$,

$\mathbf{G} = [\rho v,\rho uv,\rho v^2+p,(E+p)v,\rho Y_i v]^T$,

$\mathbf{F_v} = [0,\sigma_x,\tau_{xy},\sigma_x u + \tau_{yx} v + q_x,\dot{m}_x]^T$, and

$\mathbf{G_v} = [0,\tau_{yx},\sigma_y,\tau_{xy} u + \sigma_y v + q_y,\dot{m}_y]^T$.

The following terms are expressed as,

$$\sigma_x = \lambda\left(\frac{\partial u}{\partial x}+\frac{\partial v}{\partial y}\right)+2\mu\left(\frac{\partial u}{\partial x}\right),$$

$$\sigma_y = \lambda\left(\frac{\partial u}{\partial x}+\frac{\partial v}{\partial y}\right)+2\mu\left(\frac{\partial v}{\partial y}\right),$$

$$\tau_{xy} = \tau_{yx} = \mu\left(\frac{\partial u}{\partial y}+\frac{\partial v}{\partial x}\right),$$

$$q_x = \kappa\frac{\partial T}{\partial x} + \rho\sum_{j=1}^{ns} D_j H_j \frac{\partial Y_j}{\partial x},$$

$$q_y = \kappa\frac{\partial T}{\partial y} + \rho\sum_{j=1}^{ns} D_j H_j \frac{\partial Y_j}{\partial y}.$$

$$\dot{m}_{ix} = \rho D_i \frac{\partial Y_i}{\partial x}, \quad \dot{m}_{iy} = \rho D_i \frac{\partial Y_i}{\partial y}, \quad \lambda = -\frac{2}{3}\mu.$$

The values of C_p and H are considered as functions of temperature and determined from the polynomial curve fitting developed by Moss [12]. The details of transport properties and other different parameters are shown in Ali et al. [8]. Temperature is calculated by Newton-Raphson method from energy equation. The fluid dynamics is solved using an explicit Harten-Yee Non-MUSCL Modified-flux-type TVD scheme proposed by Yee [13~14]. The backward-facing step makes the flowfield turbulent at the present Mach number. Particularly, the recirculations in both upstream and downstream of injector, shocks, and expansion of both main stream and side jet leads us to use a turbulence model. Therefore, to calculate eddy viscosity we selected the zero-equation turbulence model proposed by Baldwin and Lomax [15]. The model is modified so that it can avoid the necessity for finding the edge of the boundary layer. This has been very helpful because at the injection port and adjacent region it is difficult to define boundary layer thickness. According to the model the eddy viscosity μ_t is defined as

$$\mu_t = \begin{cases} (\mu_t)_{inner} & y \le y_{crossover} \\ (\mu_t)_{outer} & y > y_{crossover} \end{cases}$$

where y is the normal distance from the wall and $y_{crossover}$ is the smallest value of y at which the value of viscosity in the outer region becomes less than or equal to the value of viscosity in the inner region. The values of the turbulent thermal conductivity of the mixture κ_t and turbulent diffusion coefficient of i-th species D_{it} are obtained from eddy viscosity coefficient μ_t by assuming a constant turbulent Prandtl and Lewis number equal to 0.91 and 1.0, respectively. They can be expressed as

$$\frac{\mu_t Cp}{k_t} = 0.91 \quad \text{and} \quad \frac{\rho D_{it} Cp}{k_t} = 1.0$$

The final values of μ, κ and D_{im} used in the governing equations are

$$\mu = \mu_l + \mu_t$$

$$\kappa = \kappa_l + \kappa_t$$

$$D_{im} = D_{iml} + D_{it}$$

where, μ_l, κ_l and D_{iml} are the viscosity coefficient, thermal conductivity and diffusion coefficient for laminar flow, respectively. More details about the turbulence model and its different parameters can be found in Ali et al. [8].

3. RESULTS AND DISCUSSION

3.1 The physics of fluid dynamics

Figures 2 shows the velocity vector in both upstream and downstream of injector. A pair of recirculation forms at the upstream of the injector; one of which is large and the other is small in size. In case 1 the recirculations are weak, which can be understood by the vector length in recirculation region. The increase of injection angle makes the recirculations stronger which can be found in cases 2 and 3. For further increase of injecting angle i. e. in cases 4 and 5 they are not significant. The large primary clockwise recirculation is caused by the backward facing step and the secondary small counter-clockwise recirculation close to injector is caused by the primary recirculation and the suction of injection. The primary recirculation increases the boundary layer thickness and the injection into a thick boundary layer causes greater penetration resulting in higher mixing. Due to interaction between main flow and side jet, the velocity of main flow decreases and the air enters the upstream recirculation. On the other hand, by diffusion and convection due to injection, the injected hydrogen enters the recirculation and mixes well with air. So upstream recirculations play a vital role on mixing and consequently cases 3 and 4 show better mixing. In downstream there is no strong recirculation in any case. Case 3 shows a very small recirculation just downstream of the injector caused by the suction of the injection and bending of the side jet. This recirculation and convection due to injection cause better mixing in case 3.

3.2 Characteristics of the flow field

The characteristics of the flow field are shown in Figs. 3, 4 and 5. Figure 3 shows the pressure distribution along the axis at 80 mm from left wall. In general, pressure in downstream near bottom wall is highest for all cases. Along vertical direction the pressure decreases up to the domain height of 2.0 cm. Above that height the pressure remains constant in cases 3~5, whereas, in cases 1 and 2 the pressure decreases near the upper boundary of the domain. Another observation is that with the increase of injection angle pressure decreases in downstream except at the upper part. This is caused by the weaker reattachment shock in downstream when injection angle is increased. Due to strong suppression of side jet in cases 1 and 2 caused by the high momentum of main flow the reattachment shock becomes stronger resulting in higher pressure in downstream. As diffusion of hydrogen is inversely proportional to the pressure, therefore, lower value of pressure indicates higher diffusion at downstream which results in greater mixing rate for the cases of higher injection angle.

Other characteristic phenomena such as seperation shock, bow shock, Mach disk, reattachment shock can be seen in figures 4 and 5. Figure 4 shows the pressure contours by which the pressure distribution and different shocks can be understood. Flow seperation is initiated by the backward facing step at left boundary. The main flow is deflected upward by the exsistance of wall at the upper part of the left boundary and the momentum of injecting flow along upward direction. The deflection angle frist increases with the increase of injection angle and then decreases for further increase of injection angle. Therefore, the deflection angle of main flow is maximum for case 3 ($\theta=90^o$) caused by the interaction of main flow with the highest momentum of injecting flow. It can be pointed out that the momentum of the injecting flow along the upward direction is maximum when the injection angle is 90° i. e. case 3. The under expanded side jet rapidly expands and forms a Mach disk and a bow shock due to the interaction with main flow. The size of the Mach disk increases with the increase of injection angle first and then decreases for higher injection angle as shown in Fig. 5. This increase of Mach disk in size is caused by higher expansion of side jet. We can see that case 2 has the highest expansion of side jet in downstream resulting in largest Mach disk among the cases considered. For the injection angle $\theta=90^o$ the slope of the bow shock is steeper indicating high iteraction between the main flow and side jet. Strong interaction causes high penetration and more uniform mixing of hydrogen in downstream. The maximum pressure and temperature in the flow field have been found immediately behind the intersection of separation shock and bow shock. The maximum temperature (in case 3, it is about 2430 K) occurs immediately behind the intersection of separation shock and bow shock. In the downstream region the reattachemnt shock is more visible in the pressure contour of Fig. 4. The reattachemnt shock starts almost at the same position of the bottom wall for all cases. The pressure is higher in the upstream recirculation region while it is much lower immediately behind the injector caused by the suction of injection.

3.3 Penetration and mixing of hydrogen

Figures 6 shows the penetration and mass concentration of hydrogen in the flow field. In this paper the term “penetration” is referred to the edge of mixing region in the vertical direction where the mole fraction of hydrogen is 5%. It can be pointed out that the penetration and mixing of hydrogen in a numerical simulation can occur by means of (i) turbulence and convection due to recirculation, and (ii) molecular diffusion. The backward facing step associated with upstream recirculation brings the injected hydrogen up to the left boundary in all cases. The hydrogen penetation height at different downstream locations can be compared from Figs. 6 (a~e). For example at 10 cm from left boundary the penetration height is up to 2 cm in case 1, whereas, it is 2.5 cm for case 2 and above 3 cm for cases 3 and 4. The penetration height of the hydrogen is higher in cases 3 and 4 (above 3 cm) indicating more uniform distribution of hydrogen and consequently higher mixing. In Figs. 6 (a~e) φ indicates the contour level of hydrogen mole fraction. The value of the minimum contour level is 0.05 and that of the maximum contour level is 1.0. The increment of adjacent higher contour level is 0.05. For all cases (case 1~5) the mole fraction contours of hydrogen are concentrated in a narrow region on the top of the injector as shown in Figs. 6 (a~e), which might become a high heat release zone in the reacting flowfield. The flame holding requires longer residence time of flame in the

burning range and this residence time strongly depends on the geometric expasion of the recirculation zone [16]. Also the equivalence ratio of fuel and oxidizer in mixture is an important factor for burning because among the mixtures, the stoichiometric mixture strength is good for combustion. Therefore, longer recirculation zone containing stoichiometric mixture strength results in a longer residence time and leads to a more stable flame. Accordingly cases 3 and 4 have good flame holding capability because they can produce larger and elongated upstream recirculation where most of the region contains good proportion of hydrogen and oxygen. Again in cases having $\theta = 30^o$ and 150^o upstream region contains lower mass cencentration of hydrogen which is not good for flame holding. In downstream hydrogen distribution is seemed to be better in cases 3 and 4 as mentiond earlier because of higher expansion of side jet.

4. CONCLUSION

In present paper the characteristics of the mixing field has been analyzed and discussed with numerical simulation of two-dimensional full Navier-Stokes equations. Taking the direction of air stream as reference, the injection angle was varied from 30° ~ 150° with 30° interval anti-clockwise. It was found that with the increase of injection angle from 30° ~ 90° mixing increased and further increment of injection angle decreased the mixing efficiency. Two competing phenomena were observed: i) in upstream of injector mixin was dominated by convection due to recirculation and ii) in downstream mixing was dominated by mass concentration of hydrogen. Small injection angle caused higher expansion of side jet resulting in higher Mach disk. The increase of injection angle decreased the down stream pressure near the side wall and increased the diffusion of hydrogen. Incorporating all the effects the configuration of moderate injection angle had the higher mixing efficiency and its upstream recirculation region with good proportion of hydrogen and oxygen might act as a good flame holder in Scramjet combustor. For the injection angle $\theta=90^o$ the slope of the bow shock is steeper indicating high interaction between the main flow and side jet. Strong interaction causes high penetration and more uniform mixing of hydrogen in downstream. The maximum pressure and temperature in the flow field was found immediately behind the intersection of separation shock and bow shock where chemical reaction might start in reacting flow field.

6. REFERENCES

1. Brown, G. L. and Roshko, A., 1974. On Density Effects and Large Structure in Turbulent Mixing Layer. J. Fluid Mechanics, vol. 64, no. 4, 575-816.
2. Papamoschou, D. and Roshko, A., 1986. Observation of Supersonic Free Shear Layers. AIAA Paper 86-0162.
3. Rogers, R. C., 1971. A Study of the Mixing of Hydrogen Injected Normal to a Supersonic Airstream. NASA TN D-6114.
4. Kraemer, G. O. and Tiwari, S. N., 1983. Interaction of Two-Dimensional Transverse Jet with a Supersonic Mainstream. NASA CR 175446.
5. Holdeman, J. D. and Walker, R. E., 1977. Mixing of a Row of Jets with a Confined Crossflow. AIAA Journal, vol. 5, no. 2.
6. Thayer III, W. J. and Corlett, R. C., 1972. Gas Dynamic and Transport Phenomena in the Two-Dimensional Jet Interaction Flowfield. AIAA Journal, vol. 10.
7. Heister, S. D., Nguyen, T. T. and Karagozian, A. R., 1989. Modeling of Liquid Jets Injected Transversely into a Supersonic Crossflow. AIAA Journal, vol. 27, no. 12, 1727-1734.
8. Ali, M., Fujiwara, T. and Leblanc, J. E., 2000. Influence of Main Flow Configuration on Mixing and Flameholding in Transverse Injection into Supersonic Airstream. Int. Journal Engineering Science, 38, 1161-1180.
9. Ali, M. and Islam, A.K.M.S., 1999. Effect of Mainflow Inlet Width on Penetration and Mixing of Hydrogen in Scramjet Combustor. Proceedings of the Eighth Asian Congress of Fluid Mechanics, pp. 647–650, December 6-10, Shenzhen, China.
10. Weidner, E.H. and Drummond, J.P., 1981. A Parametric Study of Staged Fuel Injector Configurations for Scramjet Applications. AIAA Paper 81-11468.
11. Rausch,V.L., McClinton, C.R. and Hicks, J.W., 1997. Scramjet Breath New Life into Hypersonics, Aerospace America, July, 40-46.
12. Moss, J. N., 1974. Reacting Viscous-Shock-Layer Solutions with Multicomponent Diffusion and Mass Injection. NASA TR-411.
13. Yee, H.C., 1989. A Class of High-Resolution Explicit and Implicit Shock Capturing Methods. NASA, TM 101088.
14. Yee, H. C., 1990. Upwind and Symmetric Shock-Capturing Schemes. NASA TM 89464, December.
15. Baldwin, B.S. and Lomax, H., 1978. Thin Layer Approximation and Algebraic Model for Separated Turbulent Flows. AIAA Paper 78-257.
16. Tabejamaat, S. JU. Y. and Niioka, T., 1997. Numerical Simulation of Secondary Combustion of Hydrogen Injected from Preburner into Supersonic Airflow. AIAA Journal, vol.35, no.9, September.

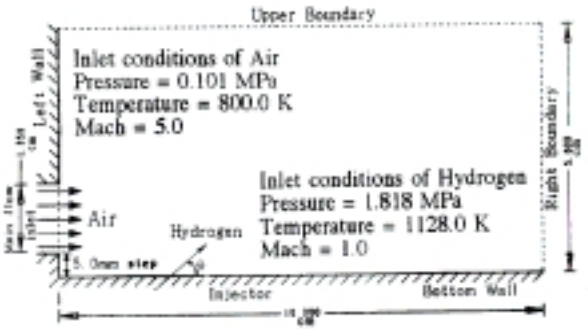

Fig.1 Schematic of physical model.
Case 1: $\theta = 30^0$, Case 2: $\theta = 60^0$,
Case 3: $\theta = 90^0$, Case 4: $\theta = 120^0$,
Case 5: $\theta = 150^0$,

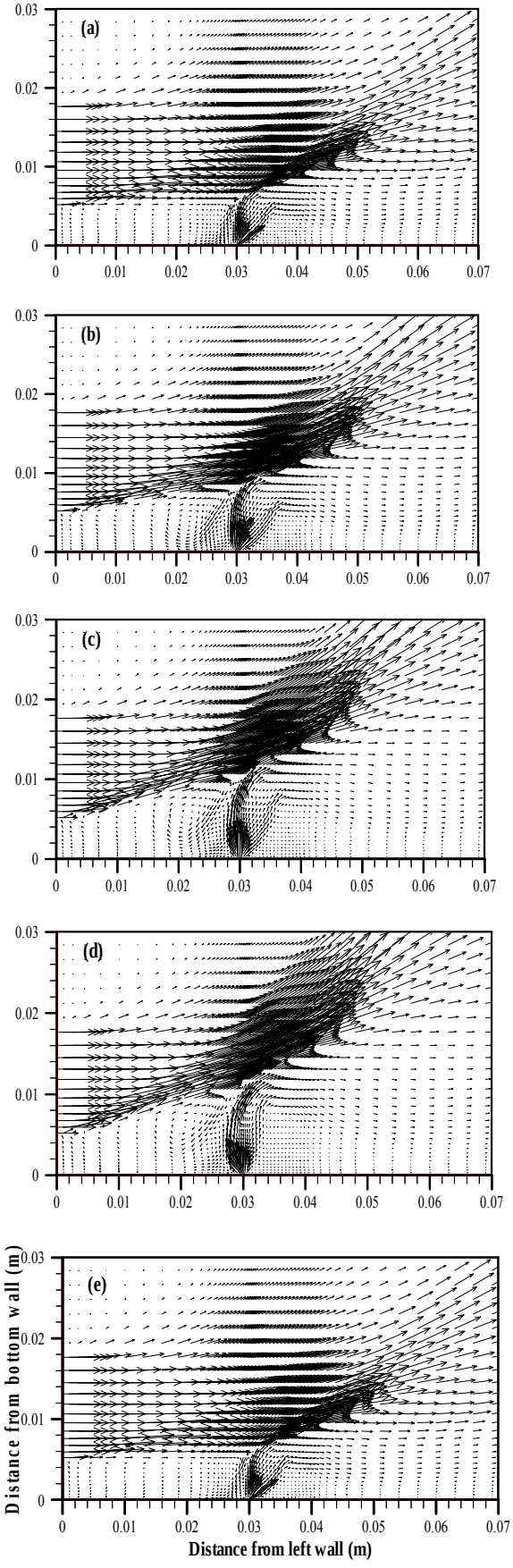

Fig.2 Velocity vector near injector; (a) Case 1, (b) Case 2, (c) Case 3, (d) Case 4, (e) Case5.

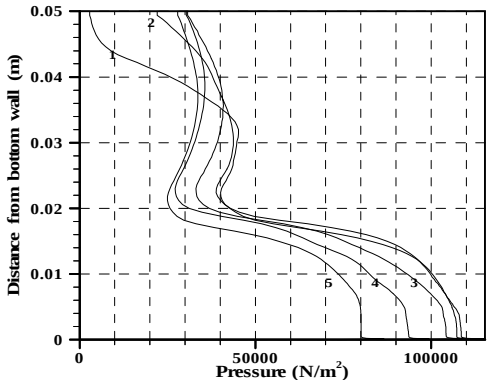

Fig.3 Pressure distribution at 8.0 cm from left wall

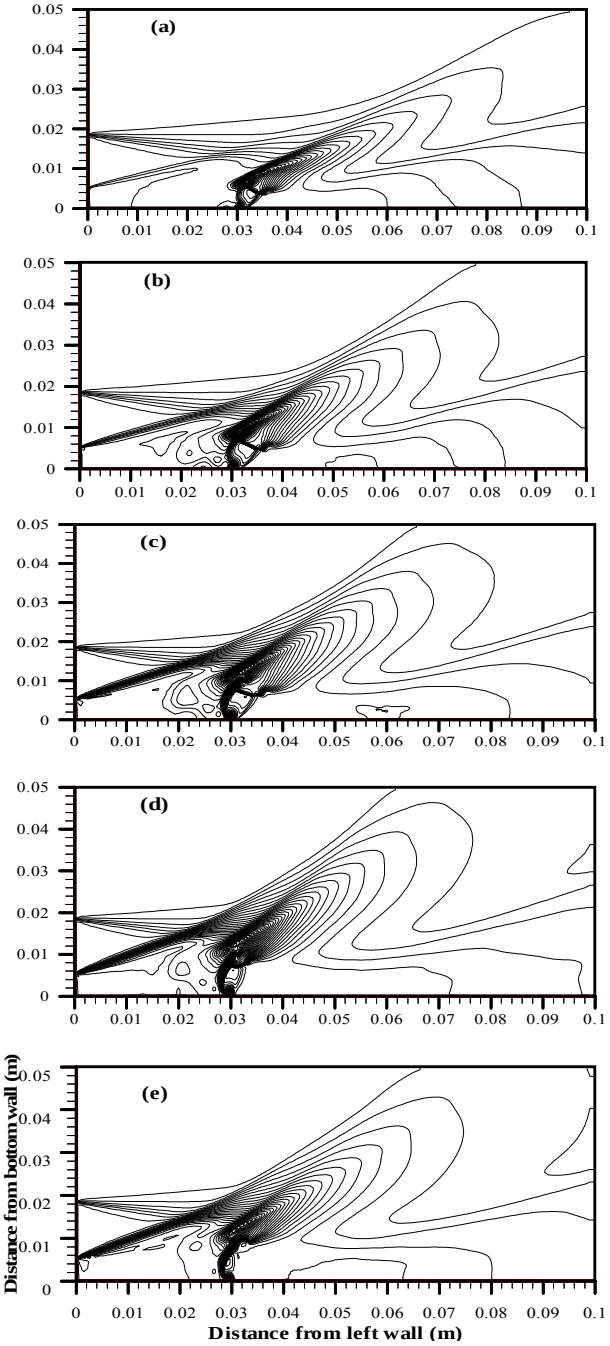

Fig.4 Pressure (N/m^2) contour, φ (2*10^4, 2*10^6, 2*10^4), φ is contour level; (a) Case 1, (b) Case 2, (c) Case 3, (d) Case 4, (e) Case 5.

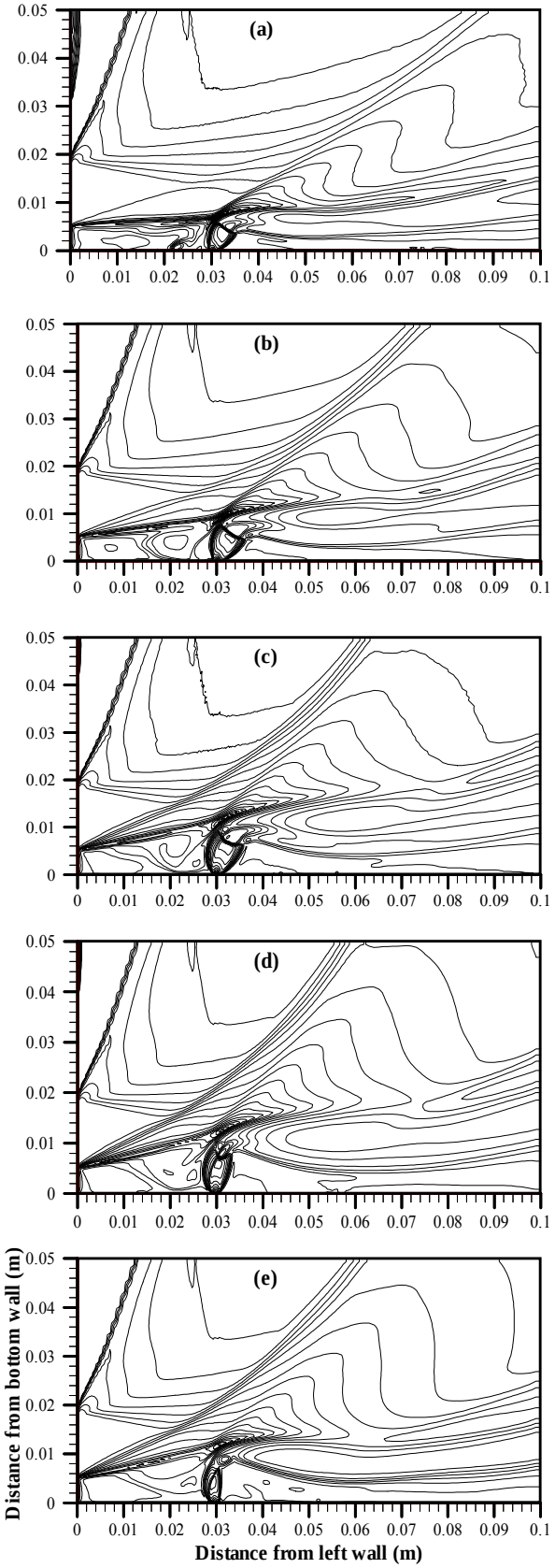

Fig.5 Temperature (K) contour, φ (250, 2550, 100), φ is contour level; (a) Case-1, (b) Case 2, (c) Case 3, (d) Case 4, (e) Case 5.

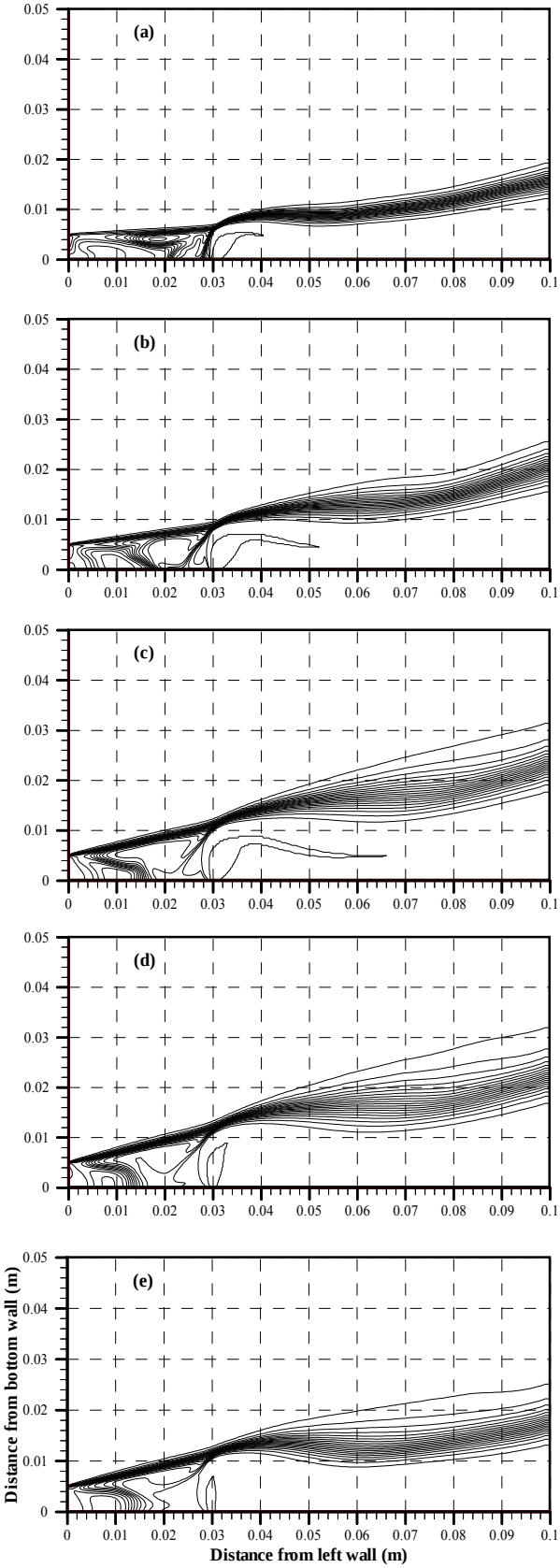

Fig.6 Mole fraction contour of Hydrogen, φ(0.05, 1.0); φ is contour level, (a) Case1, (b) Case2, (c) Case3, (d) Case4, (e) Case5